

Electronic structure of VO₂ studied by x-ray photoelectron and x-ray emission spectroscopies

E Z Kurmaev†, V M Cherkashenko†, Yu M Yarmoshenko†,
St Bartkowski‡, A V Postnikov‡, M Neumann‡, L-C Duda§, J H Guo§,
J Nordgren§, V A Perelyaev¶ and W Reichelt*

† Institute of Metal Physics, Russian Academy of Sciences – Ural Division,
Yekaterinburg GSP-170, Russia

‡ Universität Osnabrück – Fachbereich Physik, D-49069 Osnabrück, Germany

§ Physics Department, Uppsala University, Box 530, S-75121 Uppsala, Sweden

¶ Institute of Solid State Chemistry, Russian Academy of Sciences – Ural Division,
Yekaterinburg GSP-145, Russia

* Technische Universität Dresden, Institut für Anorganische Chemie, Mommsenstr.
13, D-01062 Dresden, Germany

Abstract. A VO₂ single-crystal has been subject of a combined investigation by high resolution x-ray photoelectron spectroscopy (XPS), x-ray emission spectroscopy (XES) with both electron and energy-selective x-ray excitation ($VL\alpha$ -, $VK\beta_5$ - and $OK\alpha$ -emission) and x-ray absorption spectroscopy (XAS) ($O1s$). We performed first principles tight-binding LMTO band structure calculations of VO₂ in both monoclinic and tetragonal rutile structures and compare the densities of states (DOS) with the experimental data. From this we conclude that the electronic structure of VO₂ is more bandlike than correlated.

PACS numbers: 77.84.Bw, 71.20.Be, 78.70.En, 79.60.Bm

Short title: Electronic structure of VO₂ studied by x-ray photoelectron and x-ray emission spectroscopies

October 16, 2018

1. Introduction

VO₂ belongs to transition metal compounds which exhibit metal-insulator transitions [1]. At $T=340$ K, VO₂ undergoes a phase transition from a semiconductor with monoclinic structure to a metal with the tetragonal rutile structure. The nature of the ground-state semiconducting phase is still rather uncertain. In the semiconducting phase, the V atoms are paired which was a reason for the suggestion that the electron-phonon interaction is responsible for the splitting of the d -band and the opening of a band gap [2]. This idea is supported by band structure calculations according to which the crystallographic phase transition can be explained by the formation of a charge-density wave accompanied by a lattice distortion and a subsequent condensation of phonons [3]. According to Ref. [4], there is enough energy gain to account for the metal-insulator transition through structural distortions that permits a strengthening of the vanadium d - d bonds and a reorganization of the states near the Fermi level.

On the other hand, some calculations indicate that a crystallographic distortion is not sufficient to open up a gap, and that the electron-correlation effects play an important role in the transition [5]. It was concluded in Ref. [6] that the energy gap in VO₂ is of the charge-transfer type rather than of the Mott-Hubbard type as in the late transition metal compounds, like NiO and CuO [7].

In addition to earlier spectroscopic studies [8, 9, 10, 11], the photoelectron spectroscopy measurements and low-energy electron diffraction studies on VO₂ have been carried out recently in Ref. [12, 13]. The present work aims at a combined experimental study of the electronic structure of a VO₂ single crystal at room temperature by the use of high-energy spectroscopies. A high-resolution x-ray photoelectron spectroscopy (XPS) provides information about the total density of states (DOS) in the valence band (VB); $VL\alpha$ (the $3d4s \rightarrow 2p$ transition), $VK\beta_5$ (the $4p \rightarrow 1s$ transition), $OK\alpha$ (the $2p \rightarrow 1s$ transition) x-ray emission (XES) VB spectra (excited by both electrons and photons) probe the $V3d$, $V4p$ and $O2p$ partial DOS in the valence band; the $O1s$ total electron yield spectrum probes the $O2p$ unoccupied states. Band structure calculations are performed and compared with the experimental spectra leading to the conclusion that the electronic structure of VO₂ is more bandlike than correlated.

2. Experimental procedure

The XPS measurements have been carried out with a PHI 5600 ci multitechnique spectrometer using monochromatized aluminium $K\alpha$ radiation with a full width at half-maximum (FWHM) of 0.3 eV. The energy resolution of the analyzer was 1.5% of the pass energy. We estimate an energy resolution of about 0.35 eV for the XPS measurements on VO₂. The base pressure in the vacuum chamber during the measurements was 5×10^{-9} Torr. All of the experiments presented in this paper have been performed at room temperature with the same single crystal of VO₂ ($2 \times 7 \times 0.5$ mm).

Initial measurements were performed without cleaving the crystal, and hence a high contamination of carbon was detected on the surface. Therefore the final measurements were done on a surface that was cleaved *in vacuo*. Thus an excellent surface with a relatively small amount of defects and contaminations could be obtained, and hence the intrinsic properties of the samples could be studied. For the comparison, XPS measurements of pure V metal (single crystal) were also performed.

All XPS spectra were calibrated using the Au $4f_{7/2}$ signal from an Au foil [$E_{b.e.}(4f_{7/2}) = 84.0$ eV].

Electron excited $VL\alpha$ -emission spectra (the $3d4s \rightarrow 2p_{3/2}$ transition) of VO_2 were recorded using an RSM-500 spectrometer with a diffraction grating ($N=600$ lines/mm; $R=6$ m). The accelerating voltage and current on the x-ray tube were $V=4.4$ keV and $I=0.3$ mA. The energy resolution was 0.4 eV.

$VK\beta_5$ -spectra (the $4p \rightarrow 1s$ transition) of VO_2 were measured using a fluorescent Johan-type vacuum spectrometer with a position-sensitive detector [14]. $CuK\alpha$ x-ray radiation from the sealed x-ray tube was used for excitation for the fluorescent $VK\beta_5$ XES. A quartz crystal (rhombohedral plane, second order reflection) curved to $R=1.8$ m was used as an analyzer. The spectra were measured with an energy resolution $\Delta E=0.22$ eV.

Energy-selective excited $OK\alpha$ - (the $2p \rightarrow 1s$ transition), $VL\alpha$ -spectra (the $3d4s \rightarrow 2p_{3/2}$ transition) were measured as well as x-ray absorption spectra (the $V2p$ - and $O1s$ -edges) in the sample drain-current mode. These measurements were performed at the undulator beam line BW3 at HASYLAB Hamburg, Germany [15], equipped with a modified SX-700 monochromator. The soft x-ray emission spectra were recorded at various excitation energies in the first order of diffraction with a resolution of about 0.7 eV. We used a grazing-incidence grating spectrometer [16] with an $R=5$ m spherical grating with 1200 lines/mm in a Rowland circle geometry. The resolution of the excitation radiation was set to about 1 eV by opening the exit slit of the monochromator to $400 \mu\text{m}$. The spectrometer had solid angle acceptance of about 2×10^{-5} sr, so that with a spot size of some $500 \times 500 \mu\text{m}$ at a distance of 5 cm from the entrance slit of the spectrometer we registered a maximum of about 300 counts/minute in the $VL\alpha$ line at 100 mA ring current. In order to obtain a reasonable statistical accuracy, we had to acquire for 120 to 240 minutes per single spectrum, depending on the excitation energy. The angle between the incident x-ray beam and the detection direction was 90° . This minimized the elastic scattering into the spectrometer, because the polarization of the beam coincided with the detection direction. The $V2p$ and $O1s$ absorption spectra had energy resolution of 0.2 eV for an exit slit width of $80 \mu\text{m}$. No special surface preparation was undertaken for these measurements.

3. Results and Discussion

3.1. Electronic Structure Calculations

The band-structure calculations were carried out by the tight-binding linear muffin-tin orbital method (TB-LMTO) in the atomic sphere approximation (ASA) [17], with the use of the exchange-correlation potential as parametrized by von Barth and Hedin [18] and gradient corrections as proposed by Langreth and Mehl [19] on top of the local density approximation (LDA). Since both rutile and monoclinic structures of VO_2 are relatively loosely packed, it was necessary to include empty spheres in the ASA calculations. For the tetragonal rutile phase, we used the crystal structure parameters $a=4.5546\text{\AA}$, $c/a=0.626$ and $u=0.300$ as given in Ref. [20]. Besides two formula units of VO_2 , our unit cell included eight equivalent empty spheres, which form long chains parallel to the linear O-V-O fragments, separating the latter. Due to the difference between the V and O atomic sphere radii, the chains are slightly bent. Our choice of the sphere radii S , based on the attainability of good matching

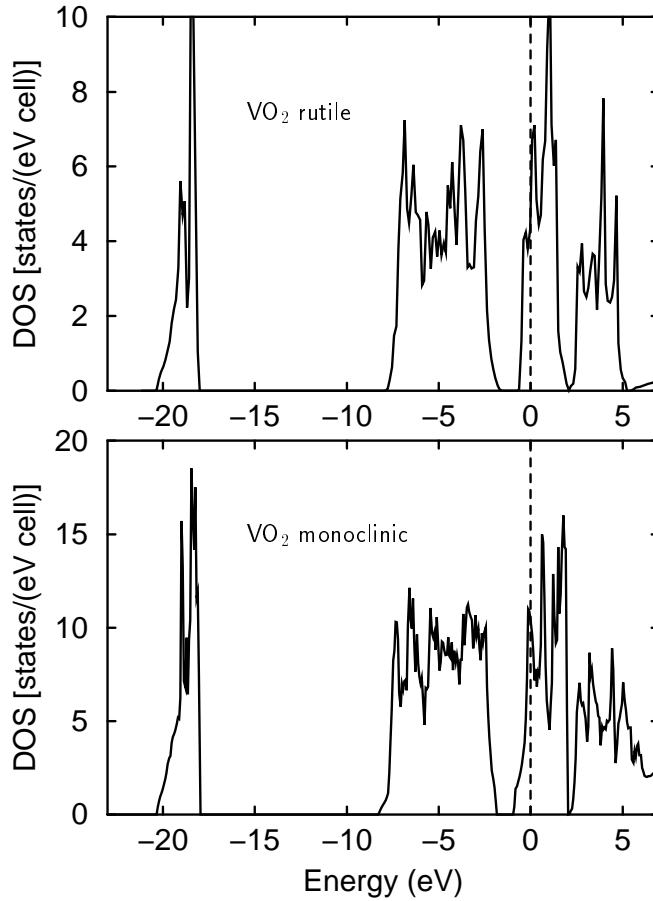


Figure 1. Total density of states calculated for rutile (tetragonal) and monoclinic crystal structures of VO_2 .

between the potential at the V and O atomic spheres compatible with a radial sphere overlap below 25% of all interatomic distances, was: $S(\text{V})=2.702$ a.u.; $S(\text{O})=1.762$ a.u.; $S(\text{empty spheres})=1.619$ a.u. The calculated band structure and the total DOS are rather close to those obtained earlier in Ref. [3, 21, 22] by different methods. We performed our own calculation because no data on the partial DOS, that are necessary for the discussion of the XES, were available from the previous calculations. Our calculated total DOS for the rutile phase of VO_2 is shown in Fig. 1, upper panel.

As is usual in oxides, the valence band is formed by hybridized transition metal $3d$ and $\text{O}2p$ states. The band gap of 0.9 eV within the valence band separates the regions where $\text{O}2p$ states (below the gap) and $\text{V}3d$ states (above the gap) dominate. The Fermi level crosses the upper subband, revealing a metallic behaviour of VO_2 , as consistent with the results of other calculations done for the rutile-type structure [3, 4, 21, 22]. The $\text{O}2s$ -related subband (which experiences some hybridization with the $\text{V}3d$ and $\text{V}4p$ states) lies separately at about 20 eV below the Fermi level. The overall shape of the band structure and of the total DOS obtained in our calculation is in

agreement with earlier results [3, 21, 22]; the width of the gap within the valence band is somewhat larger than 0.62 eV as obtained in the full potential linear augmented plane wave calculation of Ref. [22]. The gap width of 4.6 eV reported in Ref. [3] seems to be too large (probably due to the use of the Slater exchange potential) and not in agreement with the experimental positioning of individual subbands, as discussed in Ref. [21] or found in the present paper.

Since the room-temperature phase (for $T < 68^\circ\text{C}$) of VO_2 is monoclinic, the relevant comparison with experiment needs the calculation data for the latter structure. The monoclinic unit cell contains four formula units of VO_2 , and, because of the large number of atoms and low symmetry, only few calculations have been done by now. An earlier non-self-consistent calculation [23] reproduces an experimentally observable semiconductor band gap, but otherwise seems to be very inaccurate in describing the overall structure of the valence band. The analysis of the structure transformation by means of *ab initio* molecular dynamics in Ref. [4] shows that the monoclinic phase has lower energy than the rutile phase, and the equilibrium positions of the atoms are in good agreement with the experimental determination. However, the strength of the tendency for opening a gap within the valence band is underestimated within the LDA, and the flat bands in the vicinity of the Fermi level do not separate completely (see, e.g., Fig. 3 of Ref. [4]). This is also the case in our calculation, which we have carried out for the experimental monoclinic structure as specified in Ref. [24]. The change from rutile to monoclinic structure gives rise to a broadening of $\text{O}2p$ and $\text{V}3d$ bands by ~ 0.2 eV and to more pronounced splitting in the $\text{V}3d$ states of t_{2g} symmetry. In Ref.[25] it was shown that the inclusion of electron-phonon interaction (in the periodic shell model, based on the results of discrete-variational X_α cluster calculation) leads to the opening of the band gap. According to our calculation, the distortion of the nested bands due to the displacement of the atoms in the doubled-cell monoclinic structure gives rise to only small changes in the partial DOS, as compared to the rutile structure. Technically, the calculation deals with two inequivalent oxygen species and three inequivalent types of lattice-packing empty spheres of different sizes making a total of 24 sites. Our calculated total DOS for the monoclinic structure is shown in Fig. 1, lower panel, and some partial DOS are shown in Fig. 2. For comparison with XES, we did not distinguish the data for two oxygen species and show the averaged $\text{O}2s$ and $\text{O}2p$ DOS over all sites in Fig. 2, lowest panel. The densities of states are plotted for the $16 \times 16 \times 16$ mesh over the Brillouin zone.

3.2. X-ray Photoelectron Spectra

The intensity distribution of the VB XPS spectra reflects the total DOS of the VB, up to the deviations due to different atomic photoionization cross-sections. The results of the XPS measurements of single crystal VO_2 are shown in Fig. 3 and in the Table 1.

The spectral measurements on the uncleaved crystal show a large contamination with carbon. This leads to a smearing of the fine structure in the entire valence band, a broadening of subbands and the appearance of an additional subband around 12–14 eV which we attribute to transitions from $\text{C}2s$ states.

In the XPS spectra of the cleaved VO_2 crystal, a distinct narrow peak is observed around 1 eV below the Fermi level, which, according to the results of our band structure calculations (see Fig. 2), has $\text{V}3d$ character. The FWHM of this peak is about 1 eV which is less than obtained in Ref. [8, 9, 10, 11].

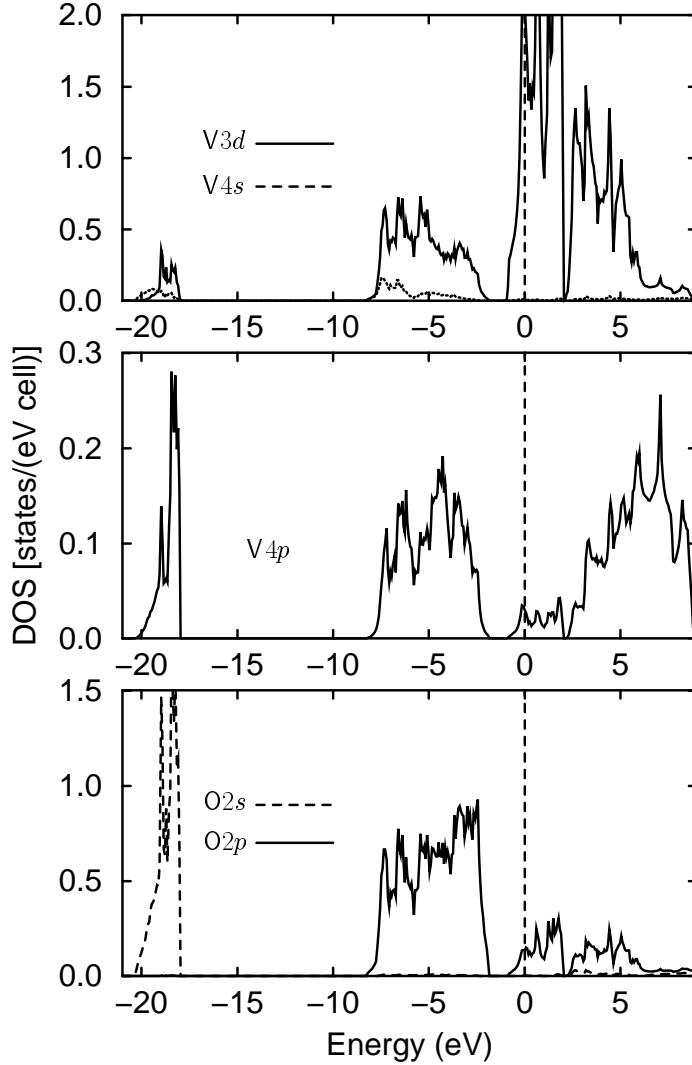


Figure 2. Partial density of states distribution in the monoclinic structure of VO_2 .

The next subband has a two-peak structure at 3–9 eV below the Fermi level which are mainly due to the $\text{O}2p$ states (*cf.* Fig. 2). Another reason for reaching this conclusion is that the energy difference between the centre of gravity of this band and the next one (located at 22 eV) is about 15 eV, which is in good agreement with the energy separation between $\text{O}2p$ and $\text{O}2s$ bands found in all vanadium oxides [26]. However, since the $\text{O}2p$ and $\text{V}3d$ atomic photoionization cross-sections for $\text{AlK}\alpha$ excitation [27] have a ratio of about 1:2, one may expect some contribution of $\text{V}3d$ states in this band. This is also confirmed by our band structure calculation and by the results from the $\text{VL}\alpha$ -emission measurements (see below). We point out, however, that there is a contradiction between the XPS and the ultraviolet photoelectron spectra (UPS) of VO_2 given in Refs. [8, 9, 10, 11, 12, 13] with respect to energy resolution and the intensity ratio of the two peaks. The peaks are well-resolved in our measurements,

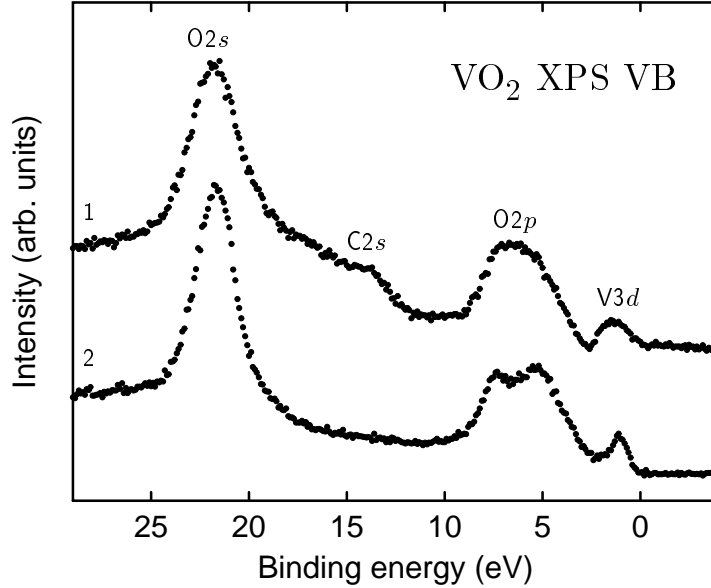


Figure 3. XPS VB spectrum of uncleaned (1) and cleaned (2) surface of VO_2 single crystal.

Table 1. XPS binding energies and width of the core levels (bands) of VO_2 .

| Core level (band) | Binding Energy (eV) | FWHM (eV) |
|--------------------|---------------------|-----------|
| $\text{V}2s$ | 630.02 | 6.10 |
| $\text{O}1s$ | 529.75 | 1.30 |
| $\text{V}2p_{1/2}$ | 523.48 | 2.56 |
| $\text{V}2p_{3/2}$ | 515.95 | 2.04 |
| $\text{V}3s$ | 68.95 | 4.54 |
| $\text{V}3p$ | 40.53 | 4.24 |
| $\text{O}2s$ | 21.73 | 2.5 |
| $\text{O}2p$ | 5.34; 7.24 | |
| $\text{V}3d$ | 1.03 | |

and both their energy separation and the intensity ratio are in good agreement with results of our band structure calculations.

According to Ref. [28], charge-transfer satellites are found in the UPS of ScF_3 , TiO_2 and V_2O_5 in the region from 11 to 17 eV below the top of the valence band. From the resonant photoemission measurements it was concluded that the charge-transfer-type configuration manifests itself in such a way as to form a valence state in the ground state in addition to the originally filled $2p$ state ligand. On the basis of this experimental evidence, cluster calculations of the valence photoemission and Bremsstrahlung isochromat spectra of VO_2 were performed in Ref. [6], and it was concluded that VO_2 belongs to the group of charge-transfer insulators. However, we point out that our XPS measurements of the uncleaned and cleaned VO_2 single crystal (Fig. 3) strongly suggest that the appearance of this structure (14-15 eV below the Fermi level) is connected with carbon contamination and that its origin is $\text{C}2s$ states.

A similar problem was discussed in Ref. [29] in connection with the analysis of UPS spectra of superconducting cuprates. There, it was concluded that the satellites with binding energies of about 10 eV are generically connected with contaminations of light elements and disappear after cleaning. Therefore we have found a clear indication that the structure in question is not an intrinsic feature of the electronic structure of pure VO_2 and cannot be considered as an evidence of correlation effects in VO_2 .

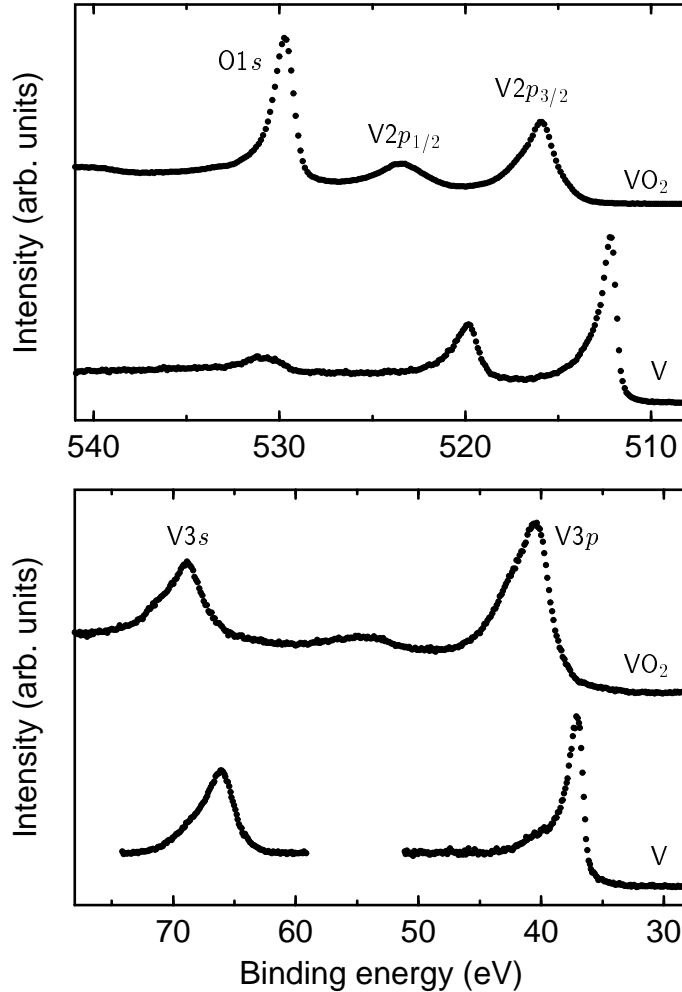


Figure 4. XPS $\text{O}1s$, $\text{V}2p_{3/2,1/2}$ (upper panel) and $\text{V}3s$, $\text{V}3p$ (lower panel) core level spectra of VO_2 and metal V .

The XPS core level spectra of VO_2 are shown in Fig. 4. The energy positions of the $\text{O}1s$, $\text{V}2p$ and $\text{V}3p$ spectra of VO_2 are close to those of Ref. [9], but the FWHM's of the lines in these spectra (see Table 1) are much smaller than it was found in Refs. [8, 9]. The lineshapes are clearly asymmetric due to a structure seen at the high-binding energy side. In case of $2p$ and $3p$ levels this may be related to np^5d^1 multiplets, as was shown in Ref. [10] for the $\text{V}3p$ spectrum. It should be noted, however, that in our measurements the $\text{V}3p$ lineshape is somewhat different from that obtained in Ref. [10].

In case of V3s level, the additional structure may be due to the exchange interaction of a (spin-up or spin-down) 3s electron left in the final state with the (V3d) electrons in the valence band[30].

In. Fig. 4, the V2p, V3s and V3p XPS core level spectra of VO₂ are compared with those of pure vanadium metal. Evidently, there is a chemical shift of the core level spectra of VO₂ with respect to that of pure metal not only for the V2p XPS-line, but also for the V3s and V3p XPS-lines. The fact that the formal charge of the vanadium atom affects V3s and V3p lines in an uniform way can be used for an estimation of the oxidation state of the V atom in compounds. Recently, the same conclusion was found for the Mn3s XPS-spectra of manganese complexes in Ref. [31].

Earlier, we have shown that the analysis of 3s XPS-spectra can be used to draw conclusions about the electronic structure of 3d metal oxides [32]. It has been found that 3s XPS-spectra of NiO have a very complicated fine structure due to charge-transfer processes. In this case, an electron may be transferred from the ligand to a metal 3d-level after the emission process, and both states, the screened and unscreened one, are visible in the 3s spectrum. The simpler fine structure of the V3s XPS-spectrum in VO₂ can be considered as an evidence for negligible charge transfer, again indicating that the electronic structure of this compound is more bandlike than correlated.

3.3. X-ray Emission Spectra

X-ray emission valence spectra result from electron transitions between the valence-band and a core hole. Since the wave function of a core electron is strongly localized and its angular momentum symmetry is well defined, these spectra reflect the site-projected and symmetry-restricted (in accordance with the dipole selection rules) partial DOS. In the case of VO₂, we have investigated VL α - (3d4s \rightarrow 2p_{3/2} transition), VK β_5 - (4p \rightarrow 1s transition) and OK α -emission spectra (2p \rightarrow 1s transition) which reflect the distribution of V3d4s, V4p and O2p partial DOS. By XPS we can measure the binding energies of the V2p and the O1s core levels so that we can determine the position of the Fermi level in the x-ray emission spectra.

The OK α and VL α spectra, adjusted in such a way as to have a a common energy scale with the X-ray photoemission spectrum, are shown in Fig. 5. The VK β_5 spectrum is positioned with respect to XPS by matching the position of the peak which results from the hybridization with O2s states. In the same figure, the partial DOS as calculated for the monoclinic phase and broadened with an energy-dependent lorentzian linewidth according to Ref. [33] are shown. Calculated and broadened partial DOS have been rigidly shifted with respect to the Fermi energy (arbitrarily, but by the same value for all spectra) to account for a systematic error in the energy matching of the measured spectra and calculated DOS due to, e.g., the absense of the band gap in the calculation.

As is seen, the main maximum of the OK α spectrum (O2p states) is placed near the top of the valence band, that is quite common in oxides, and is essentially nonbonding. A corresponding feature is also seen in the XPS but merely as a shoulder at 4 eV, due to a smaller value of O2p photoionization cross section as compared to V3d [27]. XPS VB fine sructure with two peaks at 5.4 and 7.5 eV reveals the O2p-V3d bonding band, which overlaps in energy with the maximum of the VL α spectrum and with a high-binding energy hump of the OK α spectrum.

We have excited OK α emission at two excitation energies ($E=530.8$ and 532.2

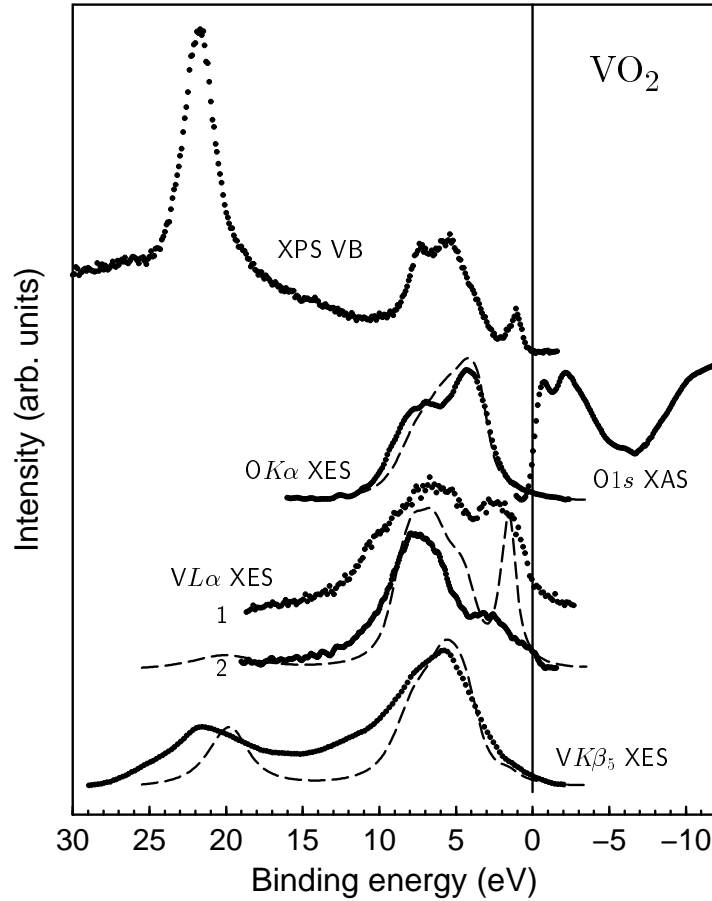


Figure 5. Dots: The comparison of XPS VB, XES ($OK\alpha$ (fluorescent excitation at $E=530.8$ eV), $VL\alpha$ (curve 1 corresponds to electron excitation at $E=4.4$ keV, curve 2 - to fluorescent excitation at $E=519.0$ eV), $VK\beta_5$ (fluorescent excitation at $E=15$ keV)) and XAS $O1s$ spectra of the VO_2 single crystal. Dashed lines: broadened partial $O2p$, $V3d$ and $V4p$ (from top to bottom) DOS as calculated for monoclinic VO_2 .

eV) which correspond to the maxima of $O1s$ x-ray absorption spectrum (XAS), but found only little difference. The $VL\alpha$ -emission spectrum has been obtained with both electron and photon excitation, that resulted in different intensity distributions (curves 1 and 2 in Fig. 5). With electron excitation at $E=4.4$ keV (curve 1), we have simultaneous excitation of $VL\alpha$ ($3d4s \rightarrow 2p_{3/2}$) and $VL\beta$ -emission ($3d4s \rightarrow 2p_{1/2}$) which are separated by only 7.53 eV. Therefore there is an overlap of the high-energy subband of $VL\alpha$ XES with the main peak of the $VL\beta$ -emission spectrum. For an excitation energy $E=519.0$ eV (curve 2), we selectively excite $VL\alpha$ which follows electron transitions from the occupied part of the $V3d$ band. From these data one can conclude that there is a considerable admixture of $V3d$ states in the $O2p$ -like bands, so that the maximum emission comes from the $V3d$ - $O2p$ hybridized band and not from an only slightly populated $V3d$ band. We find that the fine structure and energy position of the subbands of the $VL\alpha$ -emission spectrum are in reasonable agreement

with the calculated $V3d$ partial DOS distribution given in Fig. 2.

The $VK\beta_5$ -emission spectrum has two main subbands whose energy positions are very close to the $O2p$ and the $O2s$ bands due to $V4p-O2p$ and $V4p-O2s$ hybridization (see Fig. 2). The splitting of the main subband of the $VK\beta_5$ -emission spectrum also follows the calculated $V4p$ DOS distribution in this energy region. It is seen that the admixture of the $V4p$ states to the $V3d$ band is too small to be detected in the $VK\beta_5$ XES of VO_2 . The disagreement by ~ 2 eV between spectra (XPS; $VK\beta_5$) and calculated DOS in what regards the position of the $O2s$ states is known in oxides. It is related to the fact that the hole relaxation, which effectively increases the binding energy of an electron leaving a comparatively localized state such as $O2s$, is not taken into account in our band structure calculations which describe the ground state but not excitations.

It should be mentioned that soft x-ray fluorescence spectra of VO_2 ($VL\alpha, \beta$, $OK\alpha$ XES) were also recently reported in Ref. [11] and are compared with an UPS spectrum (measured at $E=501.1$ eV); however, no XPS measurements of the $V2p$ and the $O1s$ binding energies are included there. The $OK\alpha$ XES of Ref. [11] does not show the two-peak structure found in our measurements.

3.4. Total-electron-yield Spectra

$O1s$ XAS of VO_2 probes the $O2p$ unoccupied states. Such spectra, with good energy resolution, have been published earlier, by Abbate *et al.* [34]. In order to compare the XES obtained on the same samples which were used in the XPS, we include in Fig. 5 our own $O1s$ spectrum obtained (for the monoclinic phase) in the sample drain-current mode. The Fermi level has been determined with the help of the XPS binding energy of the $O1s$ level given in table 1. The $O1s$ spectrum was measured in a rather restricted energy range, so that we can only compare the spectra in the vicinity of the Fermi level.

The fine structure of the $O1s$ spectrum is in agreement with the shape of the $O2p$ conduction band in our electronic structure calculations (Fig. 2). In the high-temperature rutile phase, the calculated conduction band exhibits a pronounced two-peak structure, also discussed in Ref. [34]. In the low-temperature monoclinic phase, a further splitting of the conduction band is seen from the calculations, in agreement with a more pronounced structure in the $O1s$ spectrum of Ref. [34].

4. Conclusion

The results of measurements of high-resolution x-ray photoelectron spectra, $VL\alpha$, $VK\beta_5$ and $OK\alpha$ x-ray emission spectra (obtained by using both electron and x-ray excitation) and $O1s$ -absorption spectra of a VO_2 single crystal are presented. They are compared with first-principles LMTO band structure calculations of VO_2 in monoclinic and tetragonal rutile phases. It is concluded that the electronic structure of VO_2 is more bandlike than correlated.

5. Acknowledgements

Financial support by the Deutsche Forschungsgemeinschaft (SFB 225), the NATO (grant No. HTECH.LG971222), and the Russian Foundation for Fundamental Research (projects No 96-03-32092 and 96-15-96598) is gratefully acknowledged. One

of us (E.Z.K) wants to thank the University of Osnabrück for generous hospitality during his stay. The Uppsala group gratefully acknowledges financial support by the Swedish Natural Science Research Council (NFR) and The Göran Gustafsson Foundation and we are indebted to HASYLAB-DESY for the excellent facilities put to our disposal.

References

- [1] Adler D 1968 *Solid State Phys.* **21** 1
- [2] Goodenough J B 1960 *Phys. Rev.* **117** 1442
- [3] Gupta M, Freeman A J and Ellis D E 1977 *Phys. Rev. B* **16** 3338
- [4] Wentzcovitch R M, Schulz W W and Allen P B 1994 *Phys. Rev. Lett.* **72** 3389
- [5] Sommers C, de Groot R, Kaplan D and Zylbersztein A 1975 *J. Phys. Lett. (Paris)* **36** L157
- [6] Uozumi T, Okada K and Kotani A 1993 *J. Phys. Soc. Jpn.* **62** 2595
- [7] Zaanen J, Sawatzky G A and Allen J W 1985 *Phys. Rev. Lett.* **55** 418
- [8] Blaauw C, Leenhouts F, van der Woude F and Sawatzky G A 1975 *J. Phys. C* **8**, 459
- [9] Sawatzky G A and Post D 1979 *Phys. Rev. B* **20**, 1546
- [10] Shin S, Suga S, Taniguchi M, Fujisawa F, Kanzaki H, Fujimori A, Daimon H, Ueda Y, Kosuge K and Kachi S 1990 *Phys. Rev. B* **41**, 4993
- [11] Shin S, Agui A, Watanabe M, Fujisawa M, Tezuka Y, and Ishii T 1995 *Techn. Report of ISSP, ser. A, No. 3038*
- [12] Goering E, Schramme M, Müller O, Barth R, Paulin H, Klemm M, denBoer M L and Horn S 1997 *Phys. Rev. B* **55**, 4225
- [13] Goering E, Schramme M, Müller O, Paulin H, Klemm M, denBoer M L and Horn S 1997 *Physica B* **230-232**, 996
- [14] Dolgih V E, Cherkashenko V M, Kurmaev E Z, Goganov D A, Ovchinnikov E K and Yarmoshenko Yu M 1984 *Nucl. Instrum. Methods. Phys. Res.* **224**, 117
- [15] Pflugler J and Gurtler P 1993 *ibid.* **A287** 628
- [16] Nordgren J, Bray G, Gramm S, Nyholm R, Rubensson J E and Wassdahl N 1989 *Rev. Sci. Instrum.* **60** 1690
- [17] Andersen O K and Jepsen O 1984 *Phys. Rev. Lett.* **53** 2571; Andersen O K, Pawlowska Z and Jepsen O 1986 *Phys. Rev. B* **34** 5253
- [18] von Barth U and Hedin L 1972 *J. Phys. C* **5** 1629
- [19] Langreth D C and Mehl M J 1981 *Phys. Rev. Lett.* **47** 446; Langreth D C and Mehl M J 1983 *Phys. Rev. B* **28** 131
- [20] McWhan D B, Marezio M, Remeika J P and Dernier P D 1974 *Phys. Rev. B* **10** 490
- [21] Caruthers E, Kleinman L and Zhang H I 1973 *Phys. Rev. B* **7** 3753
- [22] Nikolaev A V, Kostubov Yu N and Andreev B N 1992 *Fiz. Tverd. Tela (St. Petersburg)* **34** 3011 [*Sov. Phys. Solid State* **34** 1614].
- [23] Caruthers E and Kleinman L 1973 *Phys. Rev. B* **7** 3760
- [24] Andersen G 1956 *Acta Chem. Scand.* **10**, 623
- [25] Nakatsugawa H and Iguchi E 1997 *Phys. Rev. B* **55** 2157
- [26] Cherkashenko V M, Kurmaev E Z, Fotiev A A and Volkov V L 1975 *Sov. Phys. Solid State* **17**, 167
- [27] Yeh J J and Lindau I 1985 *Atomic Data and Nuclear Data Tables* **32** 1
- [28] Shin S, Tezuka Y, Ishii T and Ueda Y 1993 *Solid State Commun.* **87** 1051
- [29] Takahashi T, Maeda F, Katayama-Yoshida H, Okabe Y, Suzuki T, Fujimori A, Hosoya S, Shamoto S and Sato M 1988 *Phys. Rev. B* **37** 9788
- [30] van Vleck J H 1934 *Phys. Rev.* **15** 405
- [31] Fujiwara M, Matsushita T and Ikeda S 1995 *J. Electr. Spectr. Relat. Phenom.* **74**, 201
- [32] Uhlenbrock St, Bartkowski St, Postnikov A V, Mayer B, Neumann M, Galakhov V R, Finkelstein L D, Kurmaev E Z and Leonyuk L I 1998 unpublished
- [33] Blokhin M A and Sachenko V P 1960 *Izv. Akad. Nauk SSSR, ser. fiz.* **24**, 397
- [34] Abbate M, Pen H, de Groot F M F, Fuggle J C, Ma Y J, Chen C T, Sette F, Fujimori A, Ueda Y and Kosuge K 1991 *Phys. Rev. B* **43**, 7263